

Journal of Materials Chemistry A

Accepted Manuscript



This is an *Accepted Manuscript*, which has been through the Royal Society of Chemistry peer review process and has been accepted for publication.

Accepted Manuscripts are published online shortly after acceptance, before technical editing, formatting and proof reading. Using this free service, authors can make their results available to the community, in citable form, before we publish the edited article. We will replace this *Accepted Manuscript* with the edited and formatted *Advance Article* as soon as it is available.

You can find more information about *Accepted Manuscripts* in the [Information for Authors](#).

Please note that technical editing may introduce minor changes to the text and/or graphics, which may alter content. The journal's standard [Terms & Conditions](#) and the [Ethical guidelines](#) still apply. In no event shall the Royal Society of Chemistry be held responsible for any errors or omissions in this *Accepted Manuscript* or any consequences arising from the use of any information it contains.

Title

AgPd@Pd/TiO₂ nanocatalyst synthesis by microwave heating in aqueous solution for efficient hydrogen production from formic acid†

Masashi Hattori,^a Daisuke Shimamoto,^b Hiroki Ago,^a and Masaharu Tsuji*^a

^a *Institute for Materials Chemistry and Engineering, Kyushu University, Kasuga 816-8580, Japan. E-mail tsuji@cm.kyushu-u.ac.jp*

^b *Department of Applied Science for Electronics and Materials, Graduate School of Engineering Sciences, Kyushu University, Kasuga 816-8580 Japan.*

Abstract

Ag_{100-x}Pd_x/TiO₂ ($x=7, 10, 15$) catalysts for hydrogen production from formic acid were synthesized in aqueous solution using MW heating. The hydrogen product rate of Ag_{100-x}Pd_x@Pd/TiO₂ increased concomitantly with decreasing x . The best catalytic activity was obtained for Ag₉₃Pd₇@Pd/TiO₂ ever reported among all heterogeneous catalysts.

The search for effective techniques of hydrogen gas (H_2) generation from liquid fuels has remained a difficult challenge for mobile hydrogen energy systems. Formic acid (FA) attracts great attention as such a liquid fuel because it has high energy density, nontoxicity, and excellent stability at room temperature. Moreover, FA is producible by a combination of H_2O and CO_2 with irradiation by sunlight as a primary product in artificial photosynthesis,¹⁻³ which makes FA more attractive for use in a sustainable and reversible energy storage cycle.

Some reports have described hydrogen production from the decomposition of formic acid using solid catalysts such as core-shell Au@Pd/C catalysts.^{4,5} Shortcomings of most such catalysts are high operating temperature (>80 °C) for efficient FA decomposition and reduction of catalytic activity because of CO coproduction. These shortcomings were overcome using Ag@Pd core-shell nanocatalyst, for which a high initial hydrogen rate of about $4\text{ L g}^{-1}\text{ h}^{-1}$ was achieved at room temperature without CO coproduction.⁶ The high catalytic activity of Ag@Pd core-shell nanocatalysts was explained by electron transfer from Ag core to Pd shell because of the larger work function of Pd (5.1 eV) than that of Ag (4.7 eV).⁶

We recently studied the preparation of Ag@Pd nanocatalysts loaded on TiO_2 nanoparticles using a two-step microwave-polyol method, where ethylene glycol (EG) was used as both solvent and reductant. In the first step, small Ag core particles were prepared in the presence of TiO_2 particles. Then Pd shells were synthesized in the second step. Based on spherical-aberration-corrected scanning transmission electron microscopy (STEM), STEM-energy dispersed X-ray spectroscopy (EDS), X-ray diffraction (XRD), and X-ray photoelectron spectroscopy (XPS) data, we demonstrated the preparation of Ag-Pd alloy core and Pd shell nanocrystals loaded on anatase type of TiO_2 nanoparticles (denoted as AgPd@Pd/ TiO_2). Ag and Pd atoms are partially alloyed with each other under heating above 170 °C. Therefore, $Ag_{82}Pd_{18}$ alloy and Pd shell nanocatalysts were formed. Using TiO_2 support, a higher hydrogen production rate of $16.00\pm 0.89\text{ L g}^{-1}\text{ h}^{-1}$ than that in the previous report⁶ was obtained. When we compared effects of TiO_2 support using AgPd@Pd catalysts without TiO_2 support (denoted as bare AgPd@Pd), the initial hydrogen production rate of AgPd@Pd/ TiO_2 was 23 times higher than that of bare AgPd@Pd. Significant enhancement of catalytic activity of AgPd@Pd in the presence of TiO_2 was explained by further electron transfer from TiO_2 to Pd because the work function of TiO_2 (4.0 eV) is lower than that of Pd (5.1 eV).⁷

For the practical application of AgPd@Pd/ TiO_2 catalysts, even higher activity is required. Based on previous work on catalytic activity on Ag-Pd bimetallic system,⁶ the catalytic activity of AgPd alloy catalyst was much lower than that of core-shell catalysts. These facts suggest that the catalytic activity of Ag@Pd core-shell catalysts decreases greatly by alloying between Ag core and Pd shell. Consequently, it is expected that the catalytic activity of AgPd@Pd/ TiO_2 can be greatly enhanced by dealloying AgPd core. For this purpose, a new simple method for

preparing AgPd@Pd/TiO₂ catalyst with a low Pd content in the AgPd core must be developed.

In our previous study, AgPd@Pd/TiO₂ catalysts were synthesized in EG by MW heating at 176–178 °C for about 10 min.⁷ Ag core and Pd shell were partially alloyed under heating at such a high temperature. This communication describes our attempt to prepare AgPd@Pd/TiO₂ catalysts having lower Pd content in AgPd at much lower temperature under MW heating. Here we use an aqueous solution as solvent. The reagent solution was kept at about 100 °C. The effect of alloying in AgPd core upon the catalytic activity was examined by changing the heating time used for the preparation of AgPd@Pd/TiO₂ catalysts. Results show that catalytic activity depends strongly on the extent of alloying of AgPd core. We have succeeded in the preparation of Ag_{100-x}Pd_x@Pd/TiO₂ ($x = 7, 10, 15$) catalysts having much higher catalytic activity than that of Ag₈₂Pd₁₈@Pd/TiO₂ catalysts obtained in EG.⁷

AgPd@Pd/TiO₂ was prepared using the following method. First, Ag core nanoparticles were formed in the presence of anatase type TiO₂ nanoparticles with 10 nm average diameter, synthesized by MW heating⁸ (see STEM and XRD data in Fig. S1, ESI†). Then 15 ml of distilled water containing 300 mg polyvinylpyrrolidone (PVP) and 12.26 mg AgNO₃ was mixed with the colloidal solution of 71.88 mg TiO₂ nanoparticles. The mixed solution was heated at 95 °C with MW irradiation at 120 W for 40 min under Ar bubbling. In the second step, 2 ml of distilled water containing 8.3 mg Pd(NO₃)₂ was added to this solution and heated with MW irradiation at 400 W for 30 min, 1 h, or 2 h under Ar bubbling. Typical temperature profiles of MW heating when Ag and nanoparticles and Pd shell were formed are shown in Fig. S2 (ESI†). These products are respectively called AgPd@Pd/TiO₂ (30 min), AgPd@Pd/TiO₂ (1 h), and AgPd@Pd/TiO₂ (2 h) hereinafter. The solution temperature increased to about 100 °C under MW irradiation. Characterization of product particles was conducted using STEM, STEM–EDS, XRD, XPS, and atomic absorption spectrometry (AAS). The hydrogen production rate was determined using a gas burette. Further details related to experimental methods are described in Supporting Information. Fig. S3 (ESI†) shows a typical STEM image of TiO₂ and Ag particles, where some strong white contrast Ag particles are not loaded on light contrast TiO₂ particles.

Fig. 1a–1e show STEM and STEM–EDS images of AgPd@Pd/TiO₂ (30 min). Fig. 1f shows line analysis data along the red line depicted in Fig. 1d. Results show that Ag–Pd bimetallic nanocatalysts with average diameter of 4.6±0.9 nm were loaded uniformly on TiO₂ nanoparticles and an approximately 0.8-nm-thick pure Pd shell was formed on Ag or Ag–Pd alloy core metal. The Pd/Ag atomic ratio in whole Ag–Pd bimetallic nanocatalysts was determined as 0.32±0.02 using STEM–EDS analysis. The Pd/Ag atomic ratio was also analyzed using AAS (see ESI†). The result obtained was in reasonable agreement with that estimated from the STEM–EDS analysis. STEM and STEM–EDS images of AgPd@Pd/TiO₂ (1 h) and AgPd@Pd/TiO₂ (2 h) were also observed (see Fig. S4 and S5, ESI†). These results show that

AgPd@Pd nanocatalysts of AgPd@Pd/TiO₂ (1 h) and AgPd@Pd/TiO₂ (2 h) respectively had average diameter of 4.4±0.7 nm and 4.5±1.1 nm and about 0.6-nm-thick and 0.5 nm-thick pure Pd shell. The Pd/Ag atomic ratio in whole AgPd@Pd nanocatalysts of AgPd@Pd/TiO₂ (1 h) and AgPd@Pd/TiO₂ (2 h) was determined as 0.33±0.03 and 0.31±0.01 from STEM–EDS analysis. These results show that all samples had nearly the same morphology, size, and composition, which indicates that added Pd(NO₃)₂ was reduced completely and that AgPd@Pd nanoparticles were formed by MW heating in 30 min.

Fig. 2 shows XRD patterns of AgPd@Pd/TiO₂ (30 min), AgPd@Pd/TiO₂ (1 h), and AgPd@Pd/TiO₂ (2 h) in the 2θ = 20–90° range. An expanded XRD pattern in the 2θ = 37°–40° range is shown in Fig. S6 (ESI†), where a major peak of Ag component is observed. Aside from TiO₂ anatase-peaks observed at 2θ = 25.2°, 47.9°, 53.5°, 54.9°, and 62.4° indexed to {101}, {200}, {105}, {211} and {204} facets (PDF 01-071-1168), major peaks derived from {111}, {200}, {220}, and {311} facets of Ag component of fcc Ag–Pd bimetallic particles were observed. However, these peaks slightly shift to larger 2θ from those of pure fcc Ag crystals (PDF 01-071-3762: 2θ = 38.12°, 44.31°, 64.45°, and 77.41° for {111}, {200}, {220}, and {311}, respectively). These peak shifts occur by alloying of Ag core and Pd. According to Vegard's law,⁹ which is known to be applicable to Ag–Pd systems,¹⁰ about 7.4%, 10.1%, and 15.3% of Pd atoms are dissolved respectively in AgPd alloy core particles of AgPd@Pd/TiO₂ (30 min), AgPd@Pd/TiO₂ (1 h), and AgPd@Pd/TiO₂ (2 h). Here, a weak peak was observed at 2θ = 34.4° in all samples indexed to {101} facets of PdO (PDF 01-088-2434), which was not observed in Ag–Pd particles of AgPd@Pd/TiO₂ prepared in EG solution (denoted as AgPd@Pd/TiO₂ (EG)).⁷ This result means that a small amount of PdO was formed under MW heating in aqueous solution. Moreover, the fact that the intensity ratio of the PdO {101} peak to the Ag {111} peak was AgPd@Pd/TiO₂ (1 h) > AgPd@Pd/TiO₂ (30 min) ≈ AgPd@Pd/TiO₂ (2 h) indicates that the relative amount of PdO to Ag is independent of the reaction time.

To characterize chemical states of AgPd@Pd/TiO₂ samples, XPS spectra were measured (Fig. 3a and 3b). For comparison, bare AgPd@Pd nanoparticles prepared using the same process as that of AgPd@Pd/TiO₂ (30 min) were also measured. In the XPS spectra of the 330–346 eV range (Fig. 3a), Pd 3d and PdO 3d peaks were observed in all samples. The intensity ratio of the PdO peak to the Pd peak is independent of the reaction time. These results also show that PdO was formed under MW heating in aqueous solution and the amount of PdO was not correlated with the reaction time. The Pd 3d_{5/2} and 3d_{3/2} peaks in bare AgPd@Pd shift to lower values by about 1.0 eV compared to those of pure Pd (3d_{5/2} = 335.1 eV, 3d_{3/2} = 340.3 eV) because of electron transfer from Ag to Pd arising from a difference of work functions between Ag and Pd. Similarly, the binding energies of Ag 3d_{5/2} and 3d_{3/2} peaks in bare AgPd@Pd shift to lower values by about 1.2 eV compared with those of pure Ag 3d (3d_{5/2} = 368.2 eV, 3d_{3/2} = 374.2 eV).

These binding energies were similar to those of Ag 3d peaks in Pd rich (> 90%) Ag–Pd alloy.¹¹ Therefore, it is reasonable to assume that the peak shifts originate from the formation of Ag–Pd alloy around the interface of the Ag-core and Pd-shell.

The binding energies of Pd 3d_{5/2} and 3d_{3/2} peaks of all three AgPd@Pd/TiO₂ samples were almost identical and shifted to lower values by about 0.9 eV compared to those of bare AgPd@Pd nanoparticles (3d_{5/2} = 334.2 eV, 3d_{3/2} = 339.4 eV). At the same time, the binding energies for Ag 3d_{5/2} and 3d_{3/2} peaks of all AgPd@Pd/TiO₂ samples were also almost identical and shifted to lower values by about 0.9 eV compared with those of bare AgPd@Pd nanoparticles (3d_{5/2} = 367.1 eV, 3d_{3/2} = 373.0 eV). These shifts suggest that some electrons are transferred from TiO₂ to Pd and Ag because of large differences of the work functions between Ag or Pd and TiO₂. Taking account of the fact that the binding energies for Ag and Pd are almost identical in all Ag_{100-x}Pd_x@Pd/TiO₂ (x=7, 10, 15) samples, AgPd@Pd nanoparticles were sufficiently adhered onto TiO₂ by MW heating for 30 min.

The initial H₂ production rate (R_{hydrogen}) of AgPd@Pd/TiO₂ samples was measured using the following method: total gas volume from a stirred glass tube containing 20 ml of 0.25 M aqueous formic acid and the prepared sample (metallic catalyst weight of 5.1 mg) was measured using a gas burette (see Fig. S7, ESI†). Detailed gas analyses for CO₂, H₂, and CO were performed on a gas chromatograph and no CO emission was detected using GC for all samples at 27–90 °C (see Fig. S8, ESI†). Temporal variation of total gas generation by decomposition of formic acid in the presence of Ag₉₃Pd₇@Pd/TiO₂ (30 min), Ag₉₀Pd₁₀@Pd/TiO₂ (1 h), and Ag₈₅Pd₁₅@Pd/TiO₂ (2 h) at room temperature (27 °C) is shown in Fig. 4a. The R_{hydrogen} values obtained from equations S1 and S2 of Supporting Information are presented in Table 1. For comparison, corresponding data for Ag₈₂Pd₁₈@Pd/TiO₂,⁷ bare Ag@Pd,⁶ and AuCoPd alloy nanoparticles¹² were given. The R_{hydrogen} value of Ag₉₃Pd₇@Pd/TiO₂ (30 min) sample increases greatly from 46.03 L g⁻¹ h⁻¹ at 27 °C to 371.79 L g⁻¹ h⁻¹ at 90 °C. The R_{hydrogen} value at 27 °C is about three times higher than that of Ag₈₂Pd₁₈@Pd/TiO₂ (EG) at 27 °C (16.00 L g⁻¹ h⁻¹)⁷ and about 13 and 6 times higher than those of Ag@Pd catalysts at 20 °C (3.67 L g⁻¹ h⁻¹)⁶ and CoAuPd alloy catalysts at 25 °C (7.9 L g⁻¹ h⁻¹).¹² On the other hand, the R_{hydrogen} values of Ag₉₀Pd₁₀@Pd/TiO₂ (1 h) and Ag₈₅Pd₁₅@Pd/TiO₂ (2 h) samples were, respectively 31.74 L g⁻¹ h⁻¹ and 19.17 L g⁻¹ h⁻¹ at 27 °C. Fig. 4b shows the dependence of R_{hydrogen} on the Pd contents in AgPd core. It is noteworthy that the R_{hydrogen} value increases greatly with decreasing Pd content in AgPd core and that the catalytic activity is independent of the amount of PbO which was largest in AgPd@Pd/TiO₂ (1 h). These results indicate that catalytic activity depends on the extent of alloying between Ag and Pd in AgPd core in our experimental conditions.

Hydrogen gas production rates were measured at various temperatures using AgPd@Pd/TiO₂ catalysts (Table 1). The apparent activation energies were estimated from the

following relation.

$$\ln(R_{\text{hydrogen}}) = -E_a/RT + C \quad (1)$$

In this equation, R_{hydrogen} is the initial rate of hydrogen generation, E_a is the apparent activation energy, and C is a constant. The E_a values were estimated respectively as 29.8, 32.5, and 37.8 kJ mol⁻¹ for Ag₉₃Pd₇@Pd/TiO₂ (30 min), Ag₉₀Pd₁₀@Pd/TiO₂ (1 h), and Ag₈₅Pd₁₅@Pd/TiO₂ (2 h) (see Fig. S9, ESI†). These values were higher than E_a of Ag₈₂Pd₁₈@Pd/TiO₂ prepared in EG solution (7.2 kJ mol⁻¹).⁷ The formation of PdO on the surface, which interferes with catalytic activity, might be one reason for the increase in E_a values.

In the last section we discuss on the origin of decrease in the catalytic activity with increasing x in Ag_{100-x}Pd_x@Pd/TiO₂ nanocatalysts. The atomic ratios of Pd shell to AgPd core in Ag_{100-x}Pd_x($x=7, 10, 15$)@Pd particles were estimated from STEM-EDS and XRD data to be 0.25, 0.21 and 0.15, respectively. This result suggests that the Pd/AgPd atomic ratio decreases with an increasing x . On the other hand, we found that the total Pd/Ag atomic ratio of Ag_{100-x}Pd_x@Pd/TiO₂ was nearly constant between 30 min and 2h heating. In addition, the particle sizes of Ag_{100-x}Pd_x@Pd of all samples were almost the same (≈ 4.6 nm). On the basis of above findings, reduction of Pd²⁺ on Ag or AgPd core is completed within 30 min and alloying between Ag core and Pd shell occurs between 30 min and 2h. Tsang et al.⁶ reported that Ag@Pd nanocatalysts showed their highest catalytic activity when Ag core was completely covered by thin Pd shell. The catalytic activity rapidly dropped off both when surface area of the Pd shell became low or Pd shell became thicker. It is therefore reasonable to assume that the surface area of the Pd shell of Ag_{100-x}Pd_x@Pd nanoparticles prepared in this study decreases with an increasing x because Pd atoms in Pd shell decrease owing to alloying between Ag core and Pd shell at longer MW heating.

Conclusions

For this study, we prepared Ag_{100-x}Pd_x@Pd/TiO₂ ($x=7, 10, 15$) nanocatalysts under MW heating in aqueous solution for suppressing the alloying of Ag core and Pd. The hydrogen generation rates of Ag_{100-x}Pd_x@Pd/TiO₂ ($x=7, 10, 15$) catalysts depend strongly on the degree of alloying in Ag_{100-x}Pd_x@Pd/TiO₂ catalysts. They increase by 2.4 times with decreasing the Pd content in AgPd core from 15% to 7%. The initial hydrogen formation rate of Ag₉₃Pd₇@Pd/TiO₂ (30 min) from formic acid, 46.03 L g⁻¹h⁻¹, was about three times higher than that of Ag₈₂Pd₁₈@Pd/TiO₂ (EG).⁷ To the best of our knowledge, this is the best value ever reported in the all heterogeneous catalyst.^{6,12} Our novel method for producing high catalytic

activity of core-shell AgPd@Pd nanocatalysts on TiO₂ particles in low temperature conditions is applicable for efficient hydrogen production systems intended for mobile applications.

Notes and references

^a Institute for Materials Chemistry and Engineering, Kyushu University, Kasuga, 816-8580, Japan. E-mail: tsuji@cm.kyushu-u.ac.jp

^b Department of Applied Science for Electronics and Materials, Graduate School of Engineering Sciences, Kyushu University, Kasuga 816-8580 Japan.

† This work was supported by JSPS KAKENHI Grant numbers 25286003 and 25550056, and by a Management Expenses Grant for National University Corporations from MEXT.

Electronic Supplementary Information (ESI) available. See DOI:10.1039/c000000x/

- 1 S. Sato, T. Arai, T. Morikawa, K. Uemura, T. M. Suzuki, H. Tanaka and T. Kajino, *J. Am. Chem. Soc.*, 2011, **133**, 15240–15243.
- 2 M. Mikkelsen, S. Sato, T. Kajino and T. Morikawa, *Energy and Environmental Science*, 2010, **3**, 43-81.
- 3 T. Arai, M. Jorgensen and F. C. Krebs, *Energy and Environmental Science*, 2013, **6**, 1274-1282.
- 4 X. C. Zhou, Y. Huang, W. Xing, C. Liu, J. Liao and T. Lu, *Chem. Commun.*, 2008, 3540–3542.
- 5 Y. Huang, X. Zhou, M. Yin, C. Liu and W. Xing, *Chem. Mater.*, 2010, **22**, 5122–5128.
- 6 K. Tedsree, T. Li, S. Jones, C. W. A. Chan, K. M. K. Yu, P. A. J. Bagot, E. A. Marquis, G. D. W. Smith and S. C. E. Tsang, *Nat. Nanotechnol.*, 2011, **6**, 302–307.
- 7 M. Hattori, H. Einaga, T. Daio and M. Tsuji, *J. Mater. Chem. A*, 2015, **3**, 4453-4461.
- 8 T. Yamamoto, Y. Wada, H. Yin, T. Sakata, H. Mori and S. Yanagida, *Chem. Lett.*, 2011, **38**, 964–965.
- 9 A. R. Denton and N. W. Ashcroft, *Phys. Rev. A*, 1991, **43**, 3161–3164.
- 10 L. Chen and Y. Liu, *J. Colloid Interface Sci.*, 2011, **364**, 100–106.
- 11 P. Steiner and S. Hufner, *Solid State Commun.*, 1981, **37**, 79–81.
- 12 Z.-L. Wang, J.-M., Yan, Y. Ping, H.-L. Wang, W.-T Zheng and Q. Jiang, *Angew. Chem. Int. Ed.*, 2013, **52**, 4406–4409.

Figure Captions

Fig. 1 STEM and STEM-EDS images of the AgPd@Pd/TiO₂ (30 min) nanocatalysts: (a) STEM image, (b) Ag component, (c) Pd component, (d) Ag and Pd components, (e) all components, (f) line analysis data along the red line shown in panel (e).

Fig. 2 XRD patterns of all AgPd@Pd/TiO₂ nanocatalysts.

Fig. 3 XPS spectra for all AgPd@Pd/TiO₂ nanocatalysts and bare AgPd@Pd nanocatalyst: (a) Pd 3d_{3/2,5/2} and (b) Ag 3d_{3/2,5/2}.

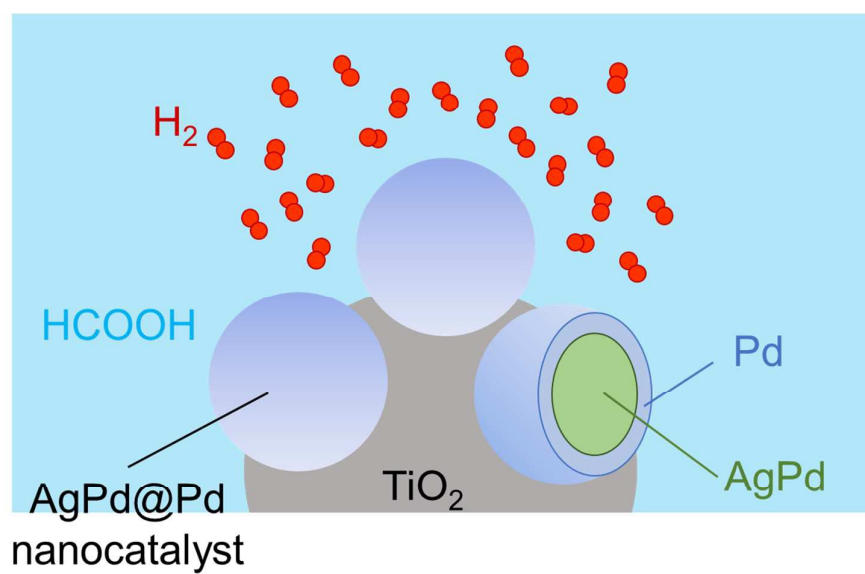
Fig. 4 (a) Gas generation by decomposition of formic acid (0.25 M, 20 mL) vs. time in the presence of AgPd@Pd/TiO₂ (30 min) nanocatalysts, AgPd@Pd/TiO₂ (1 h) nanocatalysts and AgPd@Pd/TiO₂ (2 h) nanocatalysts at 27 °C. (b) The hydrogen generation rate variation of AgPd@Pd/TiO₂ samples follows the alloying rate of Ag_{100-x}Pd_x at 27 °C.

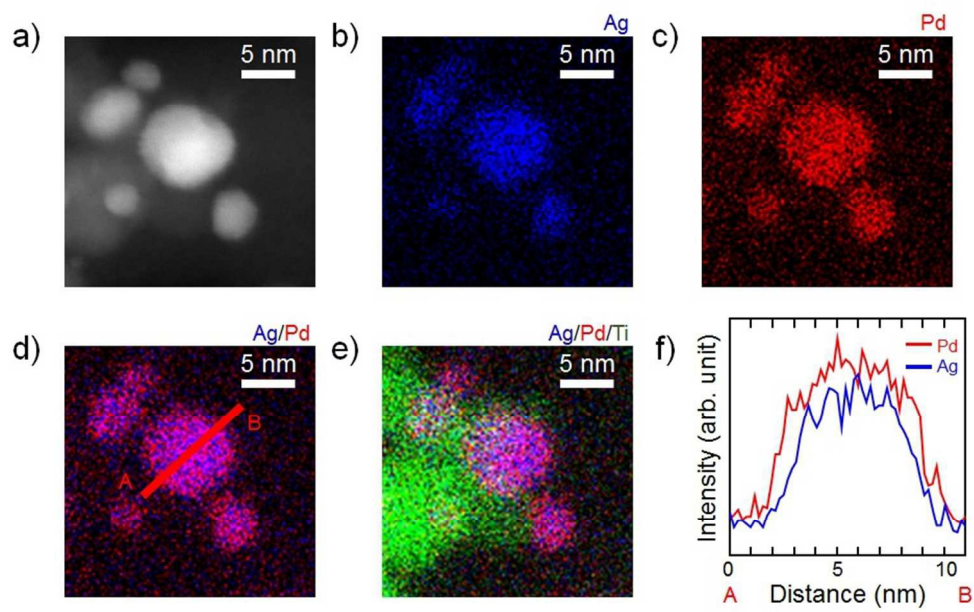
Table 1 Hydrogen production rates from catalytic decomposition of formic acid in water at different temperatures.

Catalyst	Temperature (°C)	H ₂ gas volume (L/gh)
Ag ₉₃ Pd ₇ @Pd/TiO ₂ (30 min)	27	46.03 ± 2.27
Ag ₉₃ Pd ₇ @Pd/TiO ₂ (30 min)	40	91.06 ± 4.80
Ag ₉₃ Pd ₇ @Pd/TiO ₂ (30 min)	60	143.77 ± 3.33
Ag ₉₃ Pd ₇ @Pd/TiO ₂ (30 min)	70	230.40 ± 5.69
Ag ₉₃ Pd ₇ @Pd/TiO ₂ (30 min)	90	371.79 ± 9.86
Ag ₉₀ Pd ₁₀ @Pd/TiO ₂ (1 h)	27	31.74 ± 1.64
Ag ₉₀ Pd ₁₀ @Pd/TiO ₂ (1 h)	40	57.96 ± 3.08
Ag ₉₀ Pd ₁₀ @Pd/TiO ₂ (1 h)	60	128.52 ± 5.85
Ag ₉₀ Pd ₁₀ @Pd/TiO ₂ (1 h)	70	149.06 ± 6.38
Ag ₉₀ Pd ₁₀ @Pd/TiO ₂ (1 h)	90	285.04 ± 12.01
Ag ₈₅ Pd ₁₅ @Pd/TiO ₂ (2 h)	27	19.17 ± 1.49
Ag ₈₅ Pd ₁₅ @Pd/TiO ₂ (2 h)	40	33.68 ± 0.32
Ag ₈₅ Pd ₁₅ @Pd/TiO ₂ (2 h)	60	75.85 ± 1.32
Ag ₈₅ Pd ₁₅ @Pd/TiO ₂ (2 h)	70	128.05 ± 8.22
Ag ₈₅ Pd ₁₅ @Pd/TiO ₂ (2 h)	90	253.21 ± 10.54
Ag ₈₂ Pd ₁₈ @Pd/TiO ₂ (EG) ⁷	27	16.00 ± 0.89
Ag@Pd ⁶	20	3.67
CoAuPd ¹²	25	7.9

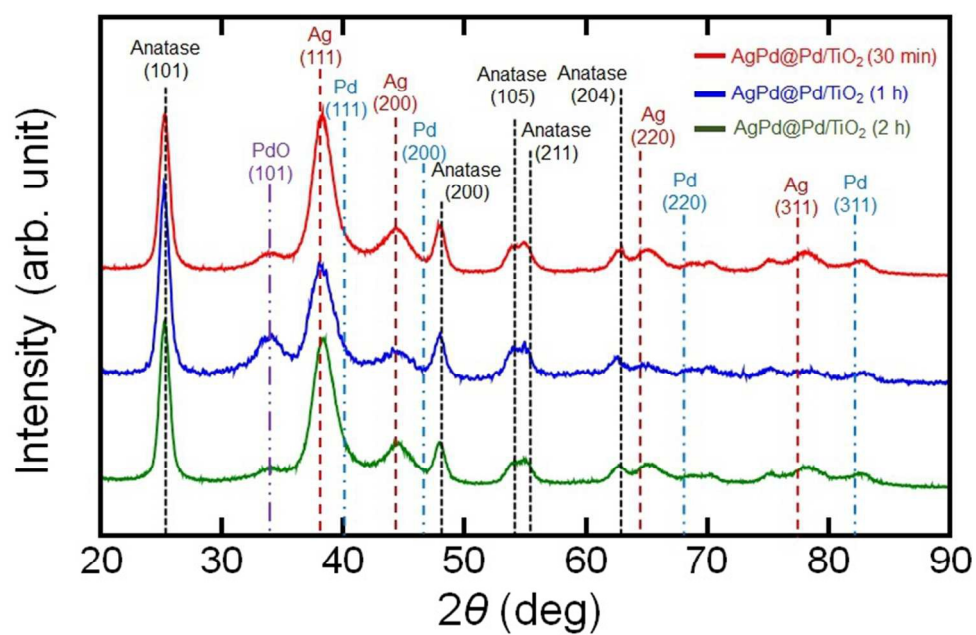
Table of contents

AgPd@Pd nanocatalysts loaded on TiO₂ were fabricated in aqueous solution using MW heating to suppress alloying for high catalytic activity.

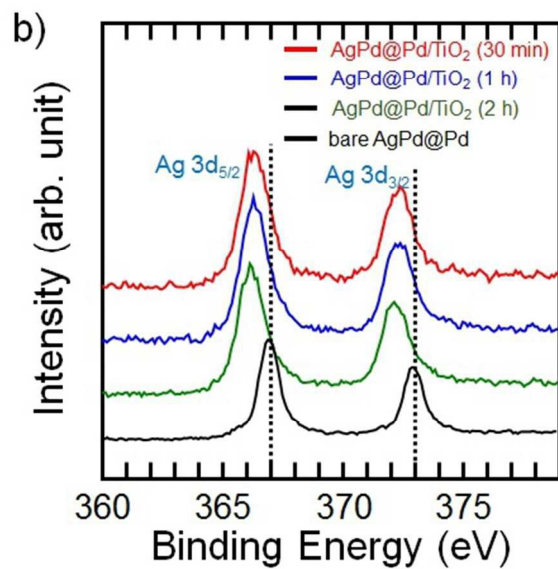
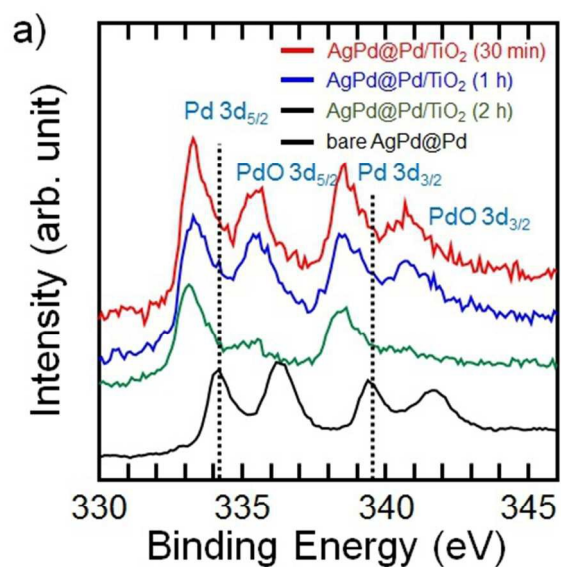




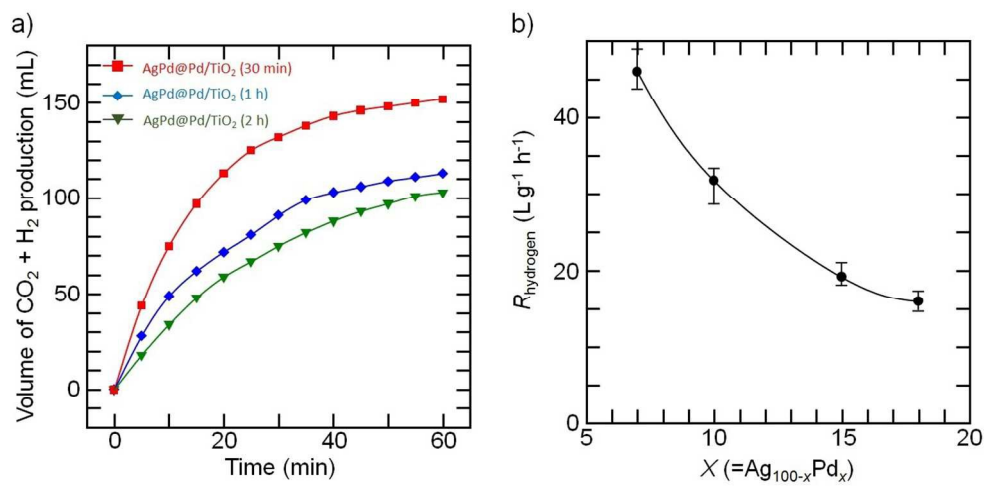
254x157mm (96 x 96 DPI)



220x145mm (96 x 96 DPI)



124x251mm (96 x 96 DPI)



365x181mm (96 x 96 DPI)